Fast Monostatic RCS Computation Using the Near-Field Sparse Approximate Inverse and the Multilevel Fast Multipole Algorithm

Carlos Delgado and Felipe Cátedra

Department of Computer Science
University of Alcalá, Alcalá de Henares, Madrid, Spain
carlos.delgado@uah.es, felipe.catedra@uah.es

Abstract ─ This paper describes an iteration-free numerical approach for the analysis of the monostatic Radar Cross Section of arbitrary scenarios. The proposed method is based on a combination of the Sparse Approximate Inverse of the near-field coupling matrix and the Multilevel Fast Multipole Algorithm, and allows to bypass the iterative solution process maintaining a good degree of accuracy.

Index Terms ─ Computational electromagnetics, inverse matrices, moment method, radar cross section.

I. INTRODUCTION

The computation of the Radar Cross Section (RCS) of complex objects has raised the interest of the academic and industrial sectors due to a wide range of applications involved. Efficient RCS computation methods can be used in approach systems, automatic vehicle identification and traffic management, collision-avoidance systems, meteorology, military applications and others. However, the calculation of the RCS of electrically large and complex objects is often restricted to the use of high-frequency methods [1] due to the relaxation of their computational requirements compared to full-wave techniques such as the Method of Moments (MoM) [2]. The use of high-frequency approaches imposes certain geometrical restrictions in order to guarantee accurate results that may not be fulfilled in some cases. Hybrid techniques [3,4,5] have typically been proposed in order to mitigate this limitation.

There has been a surge in the development of efficient full-wave approaches based on the MoM that allow to address larger problems. Some of these techniques rely on the idea of avoiding the storage of the full coupling matrix and, instead, retain only its near-field matrix, computing the interactions between distant elements using efficient matrix-vector products [6,7]. One of the most popular approaches within this group [6] is the Multilevel Fast Multipole Algorithm (MLFMA), based on the aggregation of the fields radiated by the currents over regions of the geometry to form multipole expansions that can then be translated to different points and disaggregated in order to account for distant interactions. A different strategy is based on the reduction of the number of unknowns using an extended set of basis and testing functions called macro-basis functions, which, in turn, can be seen as aggregations of the low-level functions used by the conventional MoM [8,9].

The prediction of monostatic RCS values of complex scenarios using rigorous approaches is an especially demanding task in terms of CPU-time, since it requires the solution of the matrix system for as many excitations as observation directions, although some methods have been developed in order to decrease this number using a low-rank reduction of the set of excitations [10], or the approximation of close angular monostatic values using bistatic computations [11]. A fast numerical approach developed using the two-dimensional RCS via the MLFMA combined with a low-rank spectral preconditioner and the compression of the excitation vectors using ACA is described in [12]. An alternative application of ACA for the fast computation of the monostatic RCS is shown in [13]. In [14] the authors propose a fast technique for the analysis of the monostatic RCS using Interpolative Decomposition (ID) and the skeletonization of the excitation matrix. The same algorithm is used for the analysis of wide angular sweeping in [15], overcoming the high memory requirements of the skeletonization by applying an algorithm parallelized using the Message Passing Interface (MPI) paradigm. In [16,17] extrapolations based on the Asymptotic Waveform Extraction technique (AWE) are presented for an efficient monostatic RCS computation. A Bayesian Compressive Sensing method for monostatic scattering analysis is detailed in [18]. The Best Uniform Approximation method combined with the Singular Value Decomposition (SVD) is proposed in [19] to reduce the CPU-time required for monostatic RCS computations.

We propose in this work a novel approach for the fast computation of the monostatic RCS based on the combination of the Sparse Approximate Inverse (SAI) of the near-field coupling matrix, which allows to obtain an

Submitted On: January 23, 2020
Accepted On: May 5, 2020

approximation of the currents produced by the near-field interactions between basis functions, and the MLFMA in order to take into consideration the far-field interactions. This strategy allows to bypass an iterative solution process, which generally involves most of the computing time when using a conventional full-wave solver. The accuracy obtained, as seen in the test cases provided, can be considered good for many applications while allowing to analyze problems that fall out of the scope of high-frequency techniques.

II. COMPUTATION OF THE SPARSE APPROXIMATE INVERSE

The Sparse Approximate Inverse is generally used for the generation of preconditioners in MoM-based approaches [20,21,22]. In this document we propose an alternative application, using the SAI matrix to obtain directly an initial current distribution due to the near-field interactions between basis functions. Following the conventional application of the MLFMA we assume a partitioning of the scenario in terms of cubical regions with a typical side length of λ/4.

As a starting point for the description of the analysis technique it is convenient to consider the MoM matrix equation:

$$[Z][J] = [V], \tag{1}$$

where [Z] is a non-sparse coupling matrix, [J] denotes the current density distribution to be determined and [V] is the excitation vector. It is possible to separate matrix [Z] into two parts, containing respectively the near- and far-field interactions:

$$([Z_{NF}] + [Z_{FF}])[J] = [V]. \tag{2}$$

Matrix $[Z_{NF}]$ contains the coupling terms between basis functions located in the same or in adjacent regions, which are, in turn, the coefficients with more significant magnitude. This allows to make the following approximation in order to compute its approximate inverse:

$$[Z_{NF}][J] \approx [V], \tag{3}$$

and, assuming that [M] is an approximation of the inverse of $[Z_{NF}]$, the following relation stands after performing the right multiplication of both sides by [M] in (3):

$$[J] \approx [M][V]. \tag{4}$$

In order to find [M] we impose a sparsity pattern, i.e., restrict the positions of the non-null coefficients of [M], and use a Linear Least Squares (LLS) approximation to determine the best solution that satisfies such constraint. It is common to use the same block structure of $[Z_{NF}]$ for [M] [21], although we have proposed an enlarged version of this structure based on a sparsity distance parameter [22]. The SAI matrix is computed, therefore, minimizing the norm of the difference between the identity matrix [I] and the product of [M] and $[Z_{NF}]$:

$$min\|[I] - [M][Z_{NF}]\|. \tag{5}$$

The Frobenius norm is generally applied in (5), because it allows to separate the computation of each row of the SAI matrix from the rest, which involves very good scalability properties using modern multi-core computers. By following this procedure, (5) can be decomposed into N_s independent LLS problems:

$$min\|[I] - [M][Z_{NF}]\|_F^2 = \sum_{t=1}^{N_s} min\left\|\boldsymbol{i_t} - \boldsymbol{m_t}[Z_{NF}^{(t)}]\right\|_F^2, \tag{6}$$

where N_s is the number of unknowns of the problem, $\mathbf{i_t}$ is the t-th column of the identity matrix and $\mathbf{m_t}$ makes reference to the t-th row of the SAI matrix, determined after solving the LLS problem. Matrix $[Z_{NF}^{(t)}]$ is a submatrix of $[Z_{NF}]$ obtained by discarding the coefficients that are not involved in the LLS problem. By following this procedure, after solving the N_s problems described by (6) the full SAI matrix can be obtained.

A. Filtering strategies in the SAI matrix generation

Taking into account the previous considerations regarding the matrix generation, it is possible to improve its computational efficiency as well as the memory footprint [23]. We can, on one hand, substitute matrix $[Z_{NF}^{(t)}]$ in (6) with a filtered version $[\tilde{Z}_{NF}^{(t)}]$, where the coefficients with a magnitude lower than τ times the largest self-impedance term within each MLFMA first-level region are set to 0. The τ parameter will be denoted in this work as *impedance filtering threshold*. As a result, it is possible to eliminate a number of columns in the matrix that defines each LLS problem, reducing the effective size of these problems and speeding up the SAI generation. Typical τ values of around 10^{-2} offer a noticeable CPU-time reduction while maintaining a performance comparable to that of the unfiltered version. The second filtering strategy that can be considered addresses the $\mathbf{m_t}$ solution vector in (6) that determines the t-th row of the SAI matrix. This vector, in turn, can be substituted by its filtered version $\tilde{\boldsymbol{m}}_{\boldsymbol{t}}$ in order to be stored using a reduced amount of data. In this case the filtering parameter ξ is used, denoted as *row filtering threshold*. Only the elements of the computed row with a magnitude equal or larger than ξ times that of the dominant element are to be retained, while the rest are approximated to 0. Values of 10^{-2} to $3\cdot10^{-2}$ have been proven in the existing literature [22,23] to keep good performance while requiring a fraction of the memory needed by the non-filtered SAI matrix.

III. COMPUTATION OF FAR-FIELD INTERACTIONS USING MLFMA

While the SAI matrix can be used to obtain an approximation of the current distribution on the scenario due to the near-field interactions, the MLFMA provides an operator to account for those between distant functions.

The working principle of the MLFMA consists of

aggregating the contributions of multiple basis functions to the center of their parent region. The aggregation of the j-th basis function $T_j(\vec{r'})$ to the multipole located at the center of the m-th region can be performed as follows:

$$V_{jm}^{AGG}(\hat{k}) = \int_S e^{-j\hat{k}\vec{r}_{jm}} \left(\bar{I} - \hat{k}\hat{k}\right) T_j(\vec{r'}) dS', \quad (7)$$

and, analogously, the disaggregation term of a multipole centered at the m'-th region to the i-th testing function $R_i(\vec{r'})$ can be written:

$$V_{m'i}^{DIS}(\hat{k}) = \int_S e^{j\hat{k}\vec{r}_{im'}} \left(\bar{I} - \hat{k}\hat{k}\right) R_i(\vec{r'}) dS'. \quad (8)$$

After aggregating the currents to the center of the corresponding parent regions, the multipoles can be aggregated to higher-level regions in a similar fashion and translated to other same-level regions. The translation operator $\tau_{mm'}(\hat{k}, \vec{r}_{mm'})$ allows to express the multipole expansion aggregated to the center of m as a modified multipole centered at m':

$$\tau_{mm'}(\hat{k}, \vec{r}_{mm'}) = \frac{jk}{4\pi} \sum_{l=0}^{L} j^l (2l+1) \; h_l^{(1)}(kr_{mm'}) P_l(\vec{r}_{mm'} \cdot \hat{k}), \quad (9)$$

where $h_l^{(1)}(kr_{mm'})$ is a spherical Hankel function of the first kind and $P_l(\vec{r}_{mm'} \cdot \hat{k})$ is a Legendre polynomial.

Using the aggregation of the fields radiated by the basis functions into their first-level multipoles and subsequently into their higher-level ones, the translation of the centers of these multipoles and the disaggregation it is possible perform very efficiently the matrix-vector multiplication between the far-field coupling matrix and the current vector. We will denote in this work Ψ_{FF} to the operator that allows to carry out this computation:

$$\Psi_{FF}([J]) = [Z_{FF}][J]. \quad (10)$$

IV. DESCRIPTION OF THE PROPOSED APPROACH

With the previous considerations, and after computing the SAI matrix [M] as indicated in (6), it is possible to obtain a first approximation of the current distribution on the scenario [$J^{(1)}$] multiplying the SAI matrix and the incident field vector [$V^{(1)}$]:

$$\left[J^{(1)}\right] \approx [M][V^{(1)}]. \quad (11)$$

Vector [$V^{(1)}$] in (11) is the excitation restricted to the visible zone of the geometry:

$$v_i^{(1)} = \begin{cases} v_i, if\ \hat{n}_i \cdot \hat{k} \le 0 \\ 0, if\ \hat{n}_i \cdot \hat{k} > 0 \end{cases}, \ for\ i=1..Ns, \quad (12)$$

where $v_i^{(1)}$ and v_i make reference to the i-th coefficient of [$V^{(1)}$] and [V], respectively, $\hat{k}$ is the direction of the impinging plane wave and $\hat{n}_i$ stands for the normal vector evaluated at the center of the i-th subdomain.

The field scattered by [$J^{(1)}$] can be associated, in the terminology of high-frequency approaches, to first order effects, and can be sufficient to analyze problems that do not present interactions between separate geometrical regions (such as double reflections, double diffraction or combined effects). However, in order to offer a solution for more general cases, and after obtaining [$J^{(1)}$], it is possible to calculate the field induced by this current distribution over the scenario due to the far-field contributions:

$$[V_{FF}] = \Psi_{FF}\left(\left[J^{(1)}\right]\right). \quad (13)$$

It is important to remark that [V_{FF}] requires a modification before obtaining the final induced currents. Analogously to the procedure followed in (12) it is necessary to illuminate only the visible part of the scenario, generating a new excitation vector [$V^{(2)}$] as follows:

$$v_i^{(2)} = \begin{cases} v_i^{FF}, if\ \hat{n}_i \cdot \hat{k} \le 0 \\ 0, if\ \hat{n}_i \cdot \hat{k} > 0 \end{cases}, \ for\ i=1..Ns, \quad (14)$$

where v_i^{FF} denotes the i-th coefficient of $[V_{FF}]$. It is worthwhile to remark that the current distribution [$J^{(1)}$] is equivalent to considering only the near-field coupling matrix [Z_{NF}] shown in (2), and can be refined by obtaining [$J^{(2)}$] after the introduction of the correction voltage [$V^{(2)}$] including near and far field contributions as follows:

$$[Z_{NF}]\left[J^{(2)}\right] + \left[V^{(2)}\right] = \left[V^{(1)}\right], \quad (15)$$

and an approximation of the resulting current distribution can be obtained using the SAI matrix:

$$\left[J^{(2)}\right] \approx [M]\left([V^{(1)}] - [V^{(2)}]\right). \quad (16)$$

A. SAI matrix storage and matrix-vector product strategies

In addition to the theoretical efficiency of modern computational analysis approaches, their scalability is very important in order to handle complex problems. It is necessary to make use of appropriate data structures for the concurrent generation and storage of the matrices and vectors used in the analysis. The LLS problems represented in (6) can be, thanks to the application of the Frobenius norm, distributed among a number of threads or nodes in shared-memory and distributed-memory architectures, respectively. The solution of each problem gives rise to a row of the SAI matrix. However, when distributed memory systems such as computer clusters are taken into account, there are two alternatives for the storage of this matrix: (i) each node can store the set of rows of the preconditioner that has previously computed or (ii) each row can be processed and its elements distributed to the nodes that store the corresponding parts of the current and excitation vectors. Note that the first alternative does not require exchanging messages in the SAI generation process, but needs to exchange the excitation vectors between nodes in the matrix-vector multiplications. This is the approach taken in the present work, since it requires a lesser amount of data exchanged between nodes. Figure 1 shows the matrix-vector product data distributed between a number of nodes *P* in order to clarify this situation, where each processor stores the data represented with the same color.

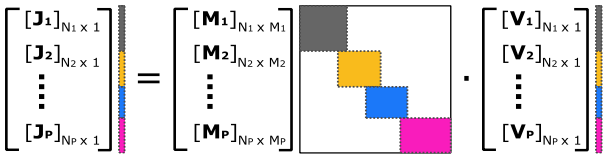

Fig. 1. Scheme illustrating the distribution of the current vector, SAI matrix and excitation vector among computing nodes, represented by blocks with different colors. N_i represents the number of rows assigned to the i-th node, while M_i corresponds to the maximum number of columns corresponding to the i-th node after applying the *row filtering threshold*.

B. Basis and testing functions applied

The scenarios considered in the present work are described by means of Non-Uniform Rational B-Spline (NURBS) surfaces defined by their (u,v) parametric coordinates. We make use of a curved mesh based on quadrangles defined on the parametric space of these patches. The basis and testing functions are rooftops and razor-blade functions defined in the parametric space. The resulting elements and functions, therefore, are curved and conformed to the surface in the real space. This scheme offers a good degree of accuracy modeling the original geometry and avoiding facetization errors. The basis functions are introduced between pairs of adjacent subdomains for the u and v components. Figure 2 depicts an example of the definition of these functions for the Electric Field Integral Equation (EFIE) formulation.

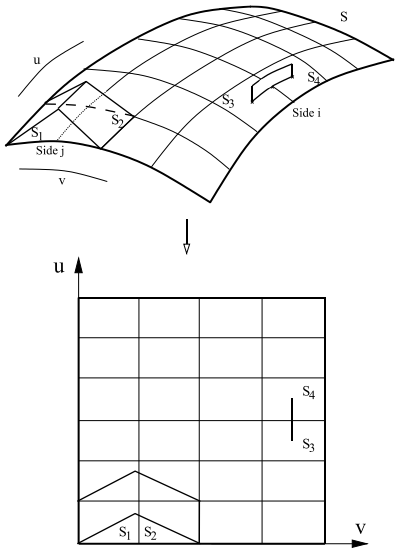

Fig. 2. Illustration of the basis (curved rooftops) and testing (curved razor-blades) functions used in the presented approach over NURBS patches, in the real space (top) and parametric space (bottom). Each junction between consecutive patches is denoted as a *side* and associated with a basis and a testing function.

V. NUMERICAL RESULTS

We present in this section some examples in order to validate the performance and efficiency of the proposed approach. The hardware platform used to obtain the results contains 2 Intel Xeon processors with a base clock speed of 2.9 GHz, 16 physical cores and 256 GB of RAM. The first test case considered is a cube with a side length of 1 m, coated with 2 mm of a material with an electric permittivity ε_r=2. The base of the cube rests on the XY plane, with its sides parallel to the reference axes. The center of the cube is located at (0.5, 0.5, 0.5), with all the units in meters. The monostatic RCS has been obtained for the θ-θ polarization considering the Electric Field Integral Equation at a frequency of 3 GHz for φ=0º and θ ranging from 0º to 90º in 0.5º steps. The results obtained with the presented technique have been compared with those returned by the full-wave MoM-MLFMA approach using the Biconjugate Stabilized Gradient solver (BiCGStab) [24] with a residual of 10^{-3} and using the same SAI matrix as a preconditioner. The *impedance filtering threshold* used in this case has been $\tau = 10^{-2}$, obtaining an average reduction of 25.2% for the size of the LLS problems required to retrieve the SAI rows. Using the same value for the *row filtering threshold* ($\xi = 10^{-2}$) we have obtained a reduction of the total size of the SAI matrix of 67.3%. Figure 3 shows good agreement between both approaches. In this case there are predominantly near-field interactions and therefore only the SAI matrix has been necessary to obtain the current distribution using the proposed approach, which means calculating the scattering field from the $[J^{(1)}]$ current distribution obtained as shown in (11). The total number of basis and testing functions has been 249,696. The CPU-time required for this computation has been 21,288 seconds in the case of the MoM-MLFMA and 894 seconds with the proposed technique, including an identical setup time of 541 seconds to obtain the near-field coupling matrix, the SAI matrix and the multipole data.

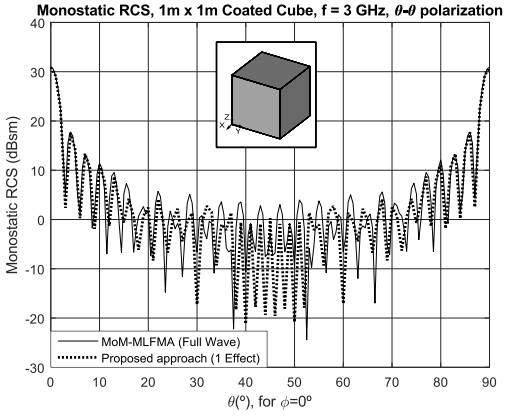

Fig. 3. Monostatic RCS results for the scenario containing a coated cube.

The second test case considered includes an additional cube, with the same characteristics as that previously described, with its center located at (-1.5, 0.5, 2.5), where all the units are expressed in meters. This case has been analyzed considering the same frequency, polarization and observation directions and includes second order effects in addition to reflection. To illustrate the difference between both we have separated the results obtained considering only the SAI matrix (1 effect) and the SAI-MLFMA contribution (2 effects). These results are shown in Fig. 4 and compared to those obtained using MoM-MLFMA, showing very good agreement. The impedance filtering threshold τ and the row filtering threshold ξ, as in the previous example, have been set to 10^{-2}, obtaining a reduction of the size of the LLS problems involved in the SAI matrix computation of 19.5% and a reduction of the total SAI matrix size of 72.3%. The number of basis functions has been 499,392. The total CPU-time with MoM-MLFMA using the same solver as in the previous case has been 53,940 seconds, while the proposed approach has required 6,122 seconds computing both effects and 5,240 seconds when considering only the near-field contribution. This time includes a setup stage of 3,513 seconds for both approaches. We have differentiated the results for both effects in Fig. 4 with the sole purpose of illustrating the contribution carried by each stage of the approach.

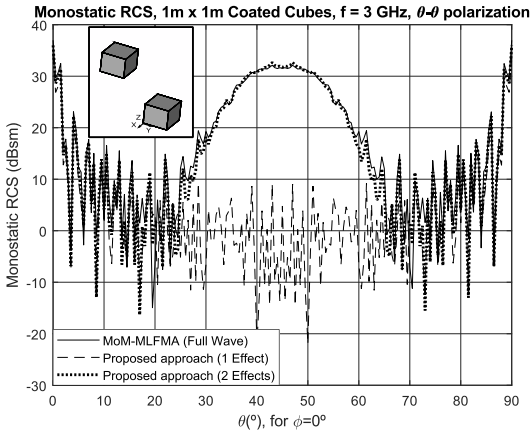

Fig. 4. Monostatic RCS results for the scenario containing two coated cubes.

VI. CONCLUSION

A novel analysis method for the computation of the monostatic RCS of arbitrary scenarios has been described in this letter. This approach presents very good efficiency compared to full-wave approaches because it does not require to make use of an iterative solver. The parametric Sparse Approximate Inverse of the near-field coupling matrix is used to obtain the induced currents considering the near-field interactions, and the Multilevel Fast Multipole Algorithm takes into account the far-field effects using the near-field derived currents in order to compute the final current distribution. Good performance and accuracy is observed in the test cases provided.

ACKNOWLEDGMENT

The work described in this letter has been supported in part by the Spanish Ministry of Economy and Competitiveness (Project Ref. TEC2017-89456-R), by the Junta de Comunidades de Castilla-La Mancha (Project Ref. SBPLY/17/180501/000433) and by the University of Alcalá (Project Ref. CCG2018/EXP-048).

REFERENCES

[1] E. F. Knott, "A progression of high-frequency RCS prediction techniques," *Proc. IEEE*, vol. 73, no. 2, pp. 252-264, Feb. 1985.

[2] R. F. Harrington, *Field Computation by Moment Methods*. New York, McMillan, 1968.

[3] D. P. Bouche, F. A. Molinet, and R. Mittra, "Asymptotic and hybrid techniques for electromagnetic scattering," *Proc. IEEE*, vol. 81, no. 12, pp. 1658-1684, Dec. 1993.

[4] L. N. Medgyesi-Mitschang and D.-S. Wang, "Hybrid methods in computational electromagnetics: A review," *Computer Physics Communications*, vol. 68, no. 1-3, pp. 76-94, Nov. 1991.

[5] C. Delgado, E. Garcia, and F. Catedra, "Hybrid iterative approach combined with domain decomposition for the analysis of large electromagnetic problems," *Proc. IEEE*, vol. 101, no. 2, pp. 320-331, Aug. 2012.

[6] W. C. Chew, J. Jin, E. Michielssen, J. Song, Ed., *Fast and Efficient Algorithms in Computational Electromagnetics*. Artech House Inc., 2001.

[7] K. Zhao, M. N. Vouvakis, J.-F. Lee, "The adaptive cross approximation algorithm for accelerated method of moments computations of EMC problems," *IEEE Trans. Electromagnetic Compat.*, vol. 14, iss. 4, pp. 763-773, Nov. 2005.

[8] E. Suter and J. R. Mosig, "A subdomain multilevel approach for the efficient MoM analysis of large planar antennas," *Micr. Opt. Technol. Letters*, vol. 26, no. 4, pp. 270-277, Aug. 2000.

[9] C. Delgado, R. Mittra, and M. F. Cátedra, "Accurate representation of the edge behavior of current when using PO-derived Characteristic Basis Functions," *IEEE Antennas and Wireless Propagation Letters*, vol. 7, no. 5, pp. 43-45, Mar. 2008.

[10] Z.-Q. Lu and X. An, "Fast monostatic radar cross-section computation for perfectly electric conducting targets using low-rank compression and adaptive integral method," *IEEE Trans. Antennas Propagat.*, vol. 52, no. 2, pp. 605-607,

Feb. 2004.
[11] M. J. Schuh, A. C. Woo, and M. P. Simon, "The monostatic/bistatic approximation," *Electromagnetics*, vol. 36, no. 4, pp. 76-78, Aug. 2004.
[12] A. Schroder, H. D. Brüns, and C. Schuster, "A hybrid approach for rapid computation of two-dimensional monostatic radar cross section problems with the multilevel fast multipole algorithm," *IEEE Trans. Antennas Propag*., vol. 60, no. 12, pp. 6058-6061, Dec. 2012.
[13] Z. Liu, R. Chen, J. Chen, and Z. Fan, "Using adaptive cross approximation for efficient calculation of monostatic scattering with multiple incident angles," *Appl. Comput. Electrom*., vol. 26, no. 4, pp. 325-333, 2011.
[14] X. M. Pan and X. Q. Sheng, "Accurate and efficient evaluation of spatial electromagnetic responses of large scale targets," *IEEE Trans. Antennas Propag*., vol. 62, no. 9, pp. 4746-4753, 2014.
[15] X. M. Pan, S. L. Huang, and X. Q. Sheng, "Wide angular sweeping of dynamic electromagnetic responses from large targets by MPI parallel skeletonization," *IEEE Trans. Antennas Propag*., vol. 66, no. 3, pp. 1619-1623, Mar. 2018.
[16] Y. E. Erdemli, J. Gong, C. J. Reddy, and J. L. Volakis, "Fast RCS pattern fill using AWE technique," *IEEE Trans. Antennas Propagat*., vol. 46, pp. 1752-1753, Nov. 1998.
[17] X. C. Wei, Y. J. Zhang, and E. P. Li, "The hybridization of fast multipole method with asymptotic waveform evaluation for the fast monostatic RCS computation," *IET Microw. Antennas Propag*., vol. 8, no. 1, pp. 46-51, Jan. 2014.
[18] H.-H. Zhang, X.-W. Zhao, Z.-C. Lin, and W. E. I. Sha, "Fast monostatic scattering analysis based on Bayesian compressive sensing," *Appl. Comput. Electrom*., vol. 31, no. 11, pp. 1279-1285, 2016.
[19] Z. Liu, S. He, X. Zhang, Y. Liu, and Y. Zhang, "Using the best uniform approximation with compression for efficient computation of monostatic scattering," *Appl. Comput. Electrom*., vol. 29, no. 11, pp. 856-863, 2014.
[20] J. Lee, J. Zhang, and C.-C. Lu, "Sparse inverse preconditioning of multilevel fast multipole algorithm for hybrid integral equations in electromagnetics," *IEEE Trans. Antennas Propagat.*, vol. 52, no. 9, pp. 2277-2287, Sept. 2004.
[21] T. Malas and L. Gürel, "Accelerating the multilevel fast multipole Algorithm with the Sparse-Approximate-Inverse (SAI) preconditioning," *SIAM J. Sci. Comput.*, vol. 31, no. 3, pp. 1968-1984, Mar. 2009.
[22] C. Delgado and M. F. Cátedra, "Sparse approximate inverse preconditioner with parametric sparsity pattern applied to Macro Basis Function methods," *IEEE Antennas and Wireless Propagation Letters*, vol. 17, no. 5, pp. 849-852, May 2018.
[23] C. Delgado, E. García, A. Somolinos, and M. F. Cátedra, "Hybrid parallelisation scheme for the application of distributed near-field sparse approximate inverse preconditioners on high-performance computing clusters," *IET Microw. Antennas Propag*., vol. 14, no. 4, pp. 320-328, Mar. 2020.
[24] G. L. G. Sleijpen and D. R. Fokkema, "Bi-CGSTAB(l) for linear equations involving unsymmetric matrices with complex spectrum," *Elec. Trans. Numer. Anal.*, vol. 1, pp. 11-32, 1993.

Carlos Delgado received the M.S. and Ph.D. degrees in Telecommunications Engineering from the University of Alcalá, Alcalá de Henares, Spain, in 2002 and 2006, respectively. He was a Visiting Scholar in 2005 and a Visiting Post-Doctoral Fellow in 2007 with the Electromagnetic Communication Laboratory, Pennsylvania State University, State College, PA, USA. He is currently an Associate Professor with the Computer Science Department, University of Alcalá. He is also a Co-Founder of newFASANT, a company that develops and commercializes electromagnetic simulation software using a wide range of numerical approaches. His current research interests include numerical methods applied to scattering and radiation problems, hybridization of high-frequency and full-wave methods, and fast computational techniques applied to electromagnetics.

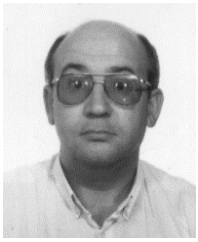

Manuel Felipe Cátedra received the M.S. and Ph.D. degrees in Telecommunications Engineering from the Polytechnic University of Madrid (UPM), Madrid, Spain, in 1977 and 1982, respectively. From 1976 to 1989 he was with the Radiocommunication and Signal Processing Department, UPM. He has been a Professor with the University of Cantabria, Santander, Spain, from 1989 to 1998. He is currently a Professor with the University of Alcalá, Madrid. He has worked on about a 100 research projects solving problems of electromagnetic compatibility in radio and telecommunication equipment, antennas, microwave components and radar cross section, and mobile communications. He has developed and applied CAD tools for radio-equipment systems such as Navy ships, aircrafts, helicopters, or satellites,

and the main contractors being EADS, ALCATEL, CNES, ALENIA, DASA, SAAB, INTA, BAZAN, INDRA, the Spanish Defense Department, CAICYT, DGICYT, CICYT, CEE (ESPRIT), European Space Agency (ESA), Ericsson, MATRA SPACE, CSELT, KTH, INAVI, Texas University, Drexel University, Singapore University, Mitsubishi, Kawasaki Heavy Industries, BOSCH, CASA, RYMSA, IRSA, INDRA, ISDEFE, TELEFONICA, ENSA, Instituto Geográfico Nacional, TELEVES, GMV, and ACCIONA. Recently, he promoted the creation of a technology-based company of the University of Alcalá called newFASANT (http://www.fasant.com) for a better transfer of techniques developed by the group.